Review of critical point symmetries and shape phase transitions within algebraic and collective models

L.Fortunato[1], C.E.Alonso[2], J.M.Arias[2], and A.Vitturi[1]
[1] *Dipartimento di Fisica e Astronomia "G.Galilei" and I.N.F.N.- Sez. Padova, via Marzolo 8, I-35131 Padova, ITALY and*
[2] *Departamento de Física Atómica, Molecular y Nuclear, Universidad de Sevilla, Apartado 1065, E-41080 Sevilla, SPAIN*

Several aspect of shape phase transitions and critical point symmstries are reviewed in this contribution within the frameworks of the Interacting Boson Model(IBM) and the Interacting Boson Fermion Model(IBFM) for even and odd sysstems respectively and compared with collective geometric models. We discuss in particular the case of an odd $j = 3/2$ particle coupled to an even-even boson core that undergoes a transition from the spherical limit $U(5)$ to the γ-unstable limit $O(6)$. The spectrum and transition rates at the critical point are similar to those of the even core and they agree qualitatively with the E(5/4) boson-fermion symmetry. We discuss also the $U^{BF}(5)$ to $SU^{BF}(3)$ shape phase transition in which the allowed fermionic orbitals are $j = 1/2, 3/2, 5/2$. The formalism of the intrinsic or coherent states is used to describe in details the ground state as well as the excited $\beta-$ and $\gamma-$bands. This formalism is also used to calculate the Potential Energy Surface of the cubic quadrupole operator that leads to traixiality.

1. Shape phase transitions

Nuclei are complex systems that can be studied with algebraic models like the IBM and IBFM or with geometric collective models, like the Bohr-Mottelson model and its extensions (for example the Frankfurth model). Although they are quantum objects they can be assigned with a specific shape (see Fig. 1) characterized by a given underlying dynamical symmetry or, more commonly, be situated somewhere along a transitional path that goes from one shape to another. Under certain approximations, at the critical point of the shape phase transition a new kind of dynamical symmetry might be found [1, 2]. This fact has been established within the Bohr-Mottelson collective approach owing to new analytic solutions of the Bohr hamiltonian [3–5] that have been applied to several nuclei and have initiated a new large chapter of research in nuclear physics. Several successful studies using the IBM have followed, because this formalism takes into account the finite number of particle and yields results that are more directly comparable with spectroscopic data. Much of this work however, has reserved attention only to even-even systems. In our activity along the years we have extended the concepts of shape phase transitions and critical point symmetries to odd nuclei within the IBFM, that allows a proper treatment of the

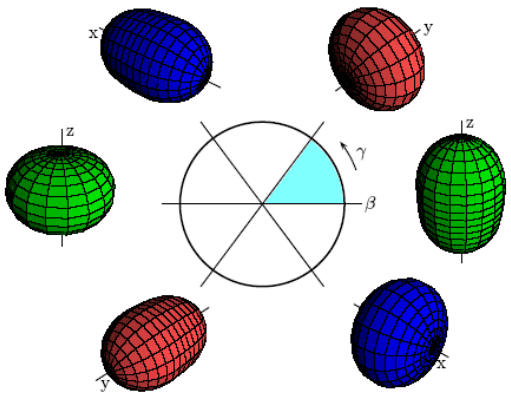

FIG. 1: Polar plane for the description of quadrupole shapes as a function of the radial variable β (quadrupole deformation) and the angle γ (asymmetry). The fundamental 60^o wedge is sufficient to describe all possible intrinsic ellipsoidal shapes because any other point in the diagram can be obtained by simply relabelling the intrinsic axes.

unpaired fermion together with the bosonic core. The formalism of the intrinsic or coherent states [8, 13] is used to describe in detail the ground state as well as the excited $\beta-$ and $\gamma-$bands and the potential energy surfaces obtained from model hamiltonians are compared with the corresponding cases proposed within the geometric collective model based on the Bohr hamiltonian.

The concept of E(5) symmetry, summarized in Fig. 2, that takes place at the critical point for the U(5)-SO(6) phase transition, has been generalized to the E(5/4) symmetry [6] in the context of the collective model. In this case the bosonic core, that undergoes a spherical to γ-unstable shape phase transition, is coupled to a fermion moving in a $j = 3/2$ orbital (that preserves the γ-independence of the total energy surface [7]). The equivalent description in the IBFM, that has a finite number of valence particles, has been given in Ref. [8]. The energy spectrum and transition rates at the critical point are shown in Fig. 3. This has been obtained with the hamiltonian

$$H = H_B + H_F + V_{BF} \,, \quad (1)$$

$$H_B = x\hat{n}_d - \frac{1-x}{N}\hat{Q}_B^{\chi=0}\cdot\hat{Q}_B^{\chi=0} \,, \quad (2)$$

which produces, varying the parameter x from 0 to 1, a transition between the two symmetries SO(6) and U(5), keeping the SO(5) symmetry untouched. The fermionic hamiltonian for a single j-shell is just a constant and can be skipped. The part that couples bosonic and fermionic degrees of freedom is $V_{BF} = -2\frac{1-x}{N}\hat{Q}_B^{\chi=0}\cdot\hat{q}_F$, where $\hat{Q}_B^{\chi=0}$ and $\hat{q}_F = (a^\dagger_{3/2}\times\tilde{a}_{3/2})^{(2)}$ are the boson and fermion quadrupole operators, respectively. The full evolution of energy levels along this transitional line is shown in Fig. 4 with all the quantum numbers that are needed to label the states. Notice that, when the odd fermion lies in an orbital that does not have $j = 3/2$, the multiplets are split (see Ref. [8, 9]). The total boson-fermion hamiltonian (1) describe the transition from Spin(6) to U(5/4), maintaining the Spin(5) symmetry along the entire transitional region. When one couples any other orbital the supersymmetric features (namely the $\gamma-$independence of the resulting potential energy surface) associated to the $j = 3/2$ orbit are lost. For example, when $j = 9/2$, the core-fermion coupling gives rise to a smoother transition than in the even-core case [9]. Fig. 5 shows the evolution of the energy surfaces along the shape phase transition (here $c = 1 - x$) for the even core and for the five components $K = 1/2, 3/2, 5/2, 7/2$ and $9/2$. One can notice that, while the core jumps into equivalent ($\gamma-$unstable) minima at the critical point, the preference of low values of K orbitals is for oblate shapes and the preference of high values of K orbitals is for prolate deformation. This fact has a simple explanation in terms of the matter distribution that results from the alignment of the angular momentum vector with the privileged z-axis. K is the same for the fermionic and total system because the bosonic part is restricted to the ground state (See Eq. (3.4) of Ref. [9]).

Another case worth mentioning is that when the fermion sits in a set of $j = 1/2, 3/2, 5/2$ orbits and it is coupled to a γ-unstable core by an appropriately chosen boson-fermion interaction, the $\gamma-$unstable character is still preserved [10]. The analytical model E(5/12) [11] for the critical point between spherical and $\gamma-$unstable has also been studied alongside with the corresponding interacting boson-fermion model [10]. This particular multi-j situation has also been investigated along the spherical to axially deformed shape phase transition [12] with the hamiltonian:

$$H = x(\hat{n}_d + \hat{n}_{3/2} + \hat{n}_{5/2}) - \frac{1-x}{4N_B}\hat{Q}_{BF}\cdot\hat{Q}_{BF} \,, \quad (3)$$

where $\hat{Q}_{BF} = \hat{Q}_B^\chi + \hat{q}_F$, $\hat{Q}_B^\chi$ is the boson quadrupole operator with $\chi = -\sqrt{7}/2$ and $\hat{q}_F$ is given in Ref. [12]. The spectrum at the critical point is shown in Fig. 6 where one can see the band structure of both the even-even and the odd-even cases: λ and μ are SU(3) quantum numbers that, strictly speaking are valid only at the limiting dynamical symmetry and not at the critical point. We use them with the label "asymptotic" as a tool to organize the band structure (see Ref. [12] for more details). Here K is the projection of

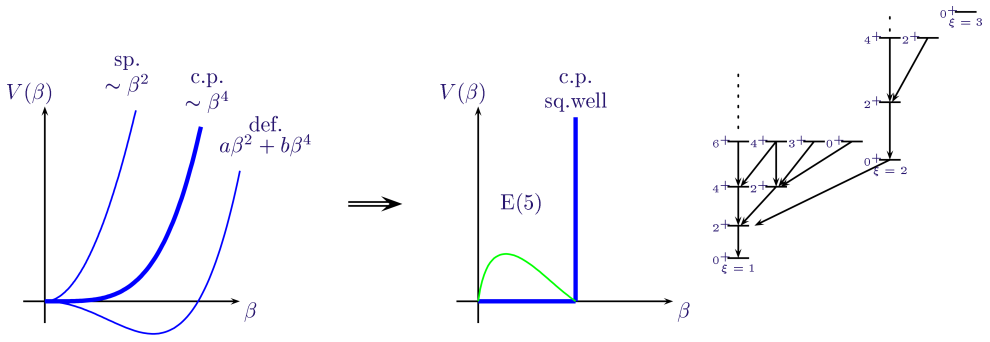

FIG. 2: The potential $V(\beta) = a\beta^2 + b\beta^4$ (left) spans from spherical to γ-unstable deformed cases, crossing the critical point (c.p.). In the E(5) solution (centre) the β^4 potential at the critical point is approximated by an infinite square well. The ground state radial wave function, which is essentially a Bessel J function is shown in green. The lower portion of the analytic spectrum of the E(5) critical point symmetry is shown on the right. The slightly anharmonic eigenstates are labelled by J^π and by a family index ξ. Arrows indicate electric quadrupole transitions.

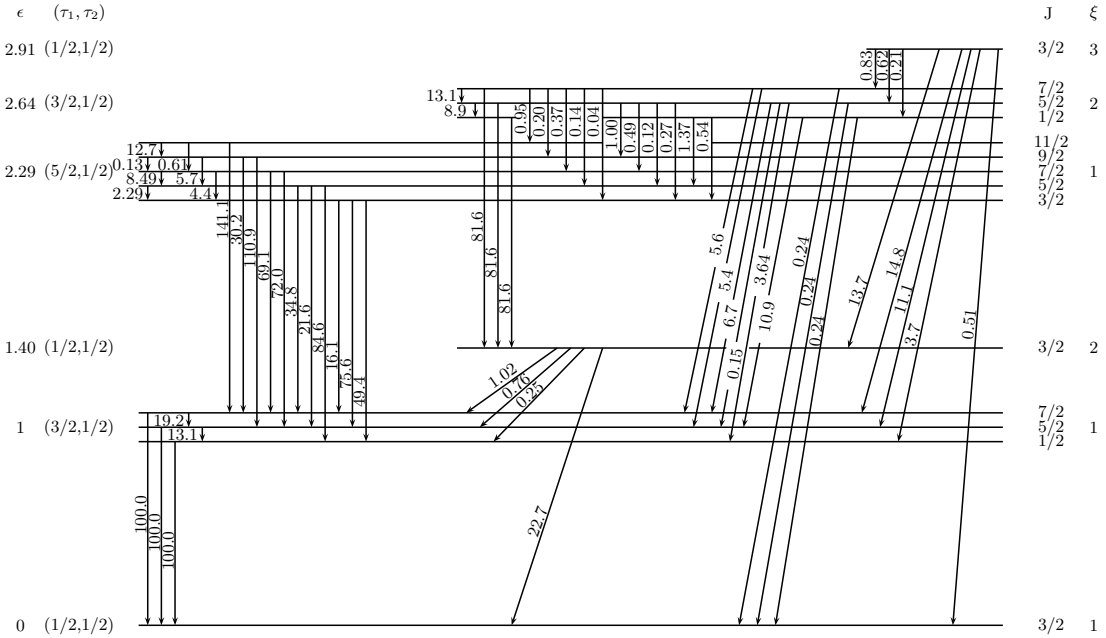

FIG. 3: Energy levels and quadrupole transition rates for the odd system (with $N = 7$ bosons and a fermion in a $j = 3/2$ orbit) at the core critical point for the spherical to $\gamma-$unstable shape phase transition (SU(5) to SO(6)). Multiplets have been arbitrarily split according to the J quantum number. Normalized energies are found in the leftmost column. States are labeled by *Spin*(5) quantum numbers, i.e. (τ_1, τ_2), spin and ξ, that labels different bands. B(E2)s have been normalized to 100 for the lowest transitions.

the core angular momentum. In the odd-even case several additional bands are present. The

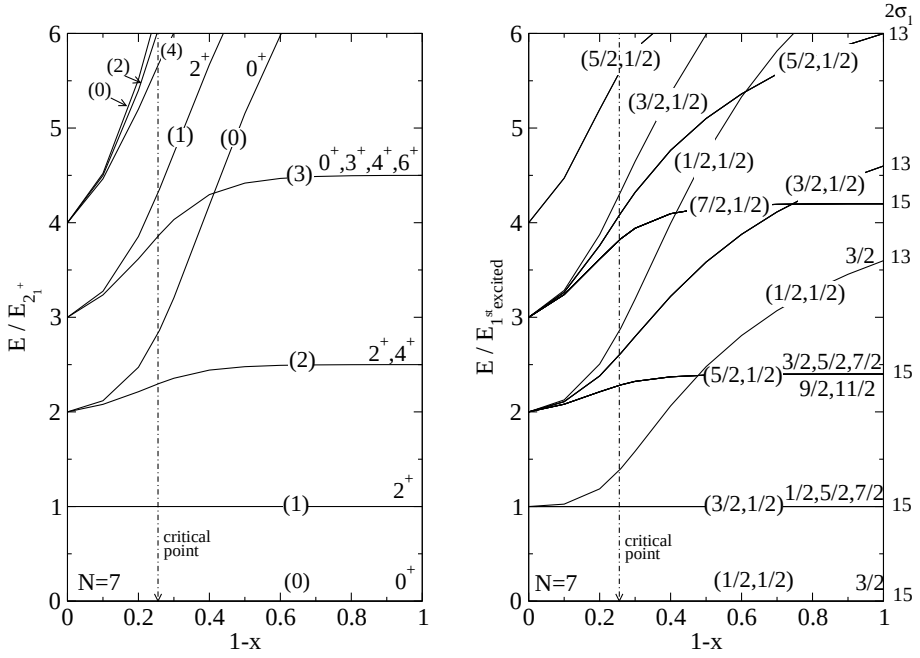

FIG. 4: Energy levels for the even and odd systems are displayed as a function of the parameter $(1-x)$ for the boson and boson-fermion Hamiltonians for the spherical to $\gamma-$unstable shape phase transition. A number N = 7 of bosons has been assumed in both cases and the odd particle has been taken in the j = 3/2 orbital. In the left panel (even case) we indicate for each level the τ quantum number, spin and parity. In the right panel we quote the (τ_1, τ_2) quantum numbers and spin. The position of the even critical point is marked.

qualitative overall look is quite similar to the corresponding even-even case. For completeness we show in Fig. 7 cuts of the odd-even (black) and even-even (violet, dashed) potential energy surfaces along $\gamma = 0$ in three cases: axially deformed dynamical symmetry, critical point of the even core and critical point of the total nucleus. The core has $N_B = 9$ bosons in all cases. All energy surfaces have been calculated within the intrinsic frame approach. They display the minimum for the same value of the deformation parameter in the leftmost panel. Here the addition of the extra particle is not changing the features of the system. At the core critical point the extra particle drives the system toward deformed or spherical shapes depending on the different which state of the odd-even nucleus we are considering. Notice how the odd-even potential energy surfaces are rather flat in the third panel that corresponds to the critical point of the odd system.

In testing and exploring the validity of critical point symmetries, other directions can be taken: for example one might want to know the predictive power of the coherent state approach to the IBM in this context. This has been tested for the ground and excited bands (i.e. the β-band in this case) far from the IBM dynamical symmetry limits in the transitional region along the γ-unstable path from U(5) to O(6) in Ref. [13]. We have found that it is a good approximation all over the transition with the exception of a narrow region close to the critical point.

In summary the salient features of shape phase transitions are quite robust with respect to the addition of an unpaired fermion,

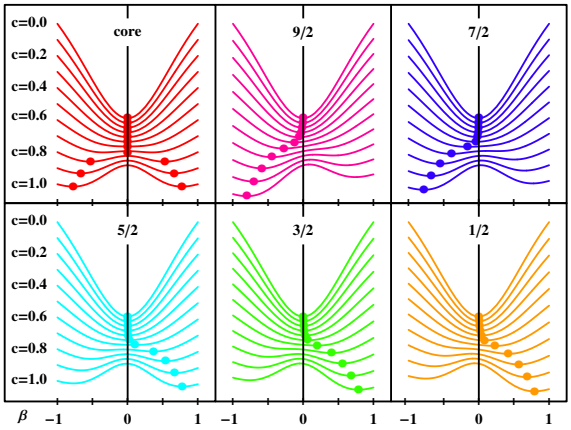

FIG. 5: Energy surfaces for the even-even core and for the different K states in the odd-even system as a function of deformation. The control parameter (c in this case correspond to $1-x$ of Eq. (2) is changed in the Hamiltonian from a spherical toward a $\gamma-$unstable shape. Cuts are along $\gamma = 0$.

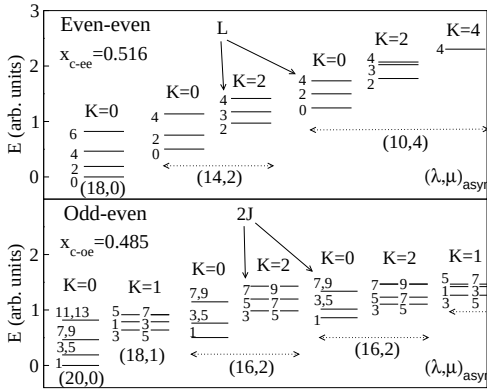

FIG. 6: Spectra at the critical points of the spherical to axially deformed shape phase transition for the the even-even case ($x_c = 0.516$) and the neighbour odd-even boson- fermion case ($x_c = 0.485$) for $N_B = 9$. Notice that the values of J are even in the first case and odd in the second, but for ease of drawing we indicate the double in the lower panel. K is the projection of the angular momentum of the core.

although, clearly, all the values of quantum numbers, excitation energies and transition rates are rather different and each case must be studied in detail to provide experimentalists with detailed predictions. In this respect,

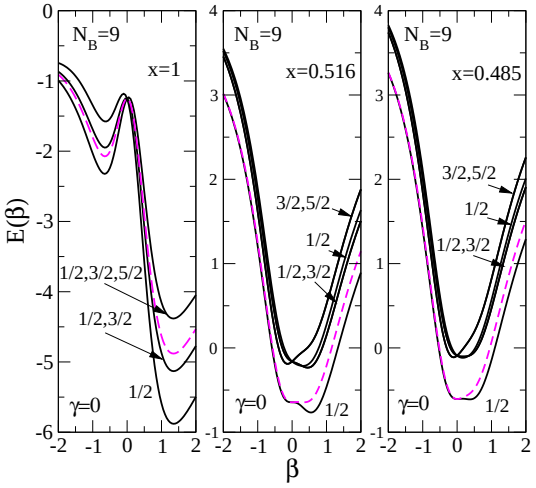

FIG. 7: Energy surfaces for different intrinsic states in the odd-even nucleus with $N_B = 9$ as a function of the deformation parameter. The dashed lines give the corresponding energy surfaces for the even-even case. The three panels correspond to different choices of the control parameter. The left panel ($x = 1$) corresponds to the $SU^{BF}(3)$ dynamical symmetry; the other panels correspond to the critical points in the even-even case ($x = 0.516$) and the odd-even case ($x = 0.485$). Cuts are along $\gamma = 0$.

we would like to stress that an extensive *corpus* of theories exists that still lacks the experimental counterpart with a few exceptions: for instance the work of Fetea et al.[14], that have performed a β-decay experiment to study the energy levels of ^{135}Ba. The results have been compared with the E(5/4) symmetry as well as with IBFM results, showing some agreement, but pointing also to discrepancies that might mean that more work on the comparison of theory and experiment is needed to establish the most important features of odd-even transitional nuclei.

Recently, Iachello, Leviatan and Petrellis have made several studies on various shape phase transitions [15] reaching essentially the same conclusions although they insist more on the fact that the position of the critical point is retarded (or anticipated) by the presence of the fermion.

2. Other studies using coherent states

We have undertaken several other studies that are based on the coherent state formalism. For example, in collaboration with I.Inci [13] we have tested the predictive power of the coherent state approach to the interacting boson model far from the IBM dynamical symmetry limits. By considering the transitional region along the γ-unstable path that leads from U(5) to O(6) we have calculated the spectrum of the excited beta-band as well as intraband and interband quadrupole electromagnetic transitions. The results of obtained with the intrinsic states are compared with the exact results as a function of the boson number N. We find that this formalism provides approximations to the exact results that are correct up to the order 1/N in the transitional region, except in a narrow region close to the critical point. In this work we have given explicit expressions for several quantities, like quadrupole moments and transition rates.

Another example is the work with R.Fossion [16] where we concentrate on two-particle transfer reactions. We study whether the evolution of the transfer spectroscopic intensities, $I(N \to N+1)$, where N is the boson number, could be used as a possible signature of shape-phase transitions, finding a positive answer. By considering chains of even-even nuclei that display analogous changes in shape, such as from spherical to axial-symmetric deformed or from spherical to deformed γ-unstable, within the IBM we find that, in correspondence to the critical points, the ground-to-ground two-particle transfer matrix elements show a rapid discontinuity (see Fig. 8). This discontinuity is associated with a corresponding increase in the transition to the excited 0+ states, a fact that could be used as a signature in the analysis of spectroscopic data. Simple formulas are

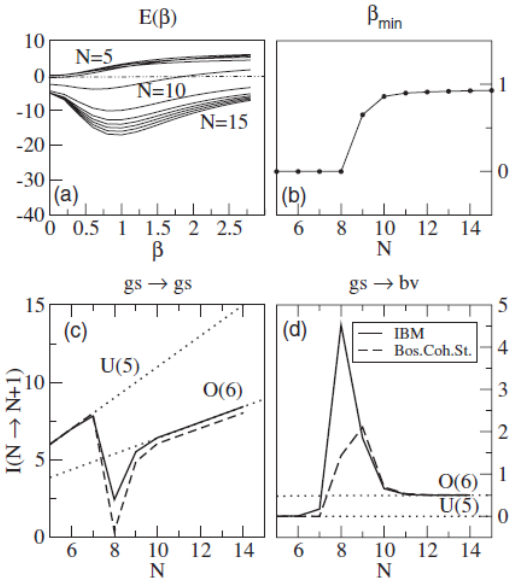

FIG. 8: Spherical to γ-unstable, U(5)-O(6), shape phase transition. (a) Cuts of PESs for $N = 515$ as a function of the quadrupole deformation β, and (b) position of the absolute minima of the different PESs. Two-particle transfer intensities calculated in the IBM (solid lines) and the boson coherent-state framework (dashed lines) are shown in (c) for the gs $\to$ gs transfer and in (d) for the gs $\to$ beta vibration transfer. The IBM predictions for the U(5) and O(6) limits are also indicated (dotted lines).

given using the intrinsic-frame formalism.

Yet another example of the profitable use that can be made of the coherent state is the work in collaboration with J.E. García-Ramos [17], where we have introduced an extension of the Interacting Boson Model that includes the cubic $(\hat{Q}\times\hat{Q}\times\hat{Q})^{(0)}$ term. We have calculated the potential energy surface, dsiplayed in Fig9 for the cubic quadrupole interaction explicitly within the coherent state formalism using the complete ($\chi-$dependent) expression for the quadrupole operator, at a variance with previous studies. This term is found to depend on the asymmetry deformation parameter γ as a linear combination of $\cos(3\gamma)$ and $\cos^2(3\gamma)$ terms, thereby allowing for the occurrence of triaxial minima in the PES of a consisten-Q formalism hamiltonian plus cubic correction. The phase diagram of the model in the large N limit is explored: the orders of the phase transition surfaces that define the phase diagram are described, and the possible nuclear equilibrium shapes are established. It is found that for this particular Hamiltonian, contrary to expectations, there is only a very tiny region of triaxiality, and that the transition from prolate to oblate shapes is so fast that, in most cases, the onset of triaxiality might go unnoticed.

To conclude this roundup of various uses of coherent states, we mention the recent study with A. Giannatiempo [18] where the the spherical to prolate deformed shape transition is studied in the framework of the interacting boson IBA-2 model, that distinguish between proton bosons and neutron bosons, by using a one-parameter Hamiltonian based on the consistent-Q hamiltonian. Excitation energies and $B(E2)$ reduced transition strengths of the ground-state, quasi-beta, and quasi-gamma bands are considered. The effects related to the finite boson number are taken into account. The IBA-2 and X(5) predictions are compared to the experimental data on 150Nd, considered one of the best examples of an X(5)- like nucleus. The analysis of potential energy surfaces of $^{144-156}$Nd, carried out in the framework of the IBA-2 model, provides further information on the structure of the neodymiun chain and the identification of the phase transition critical point.

Acknowledgments

L.F. gratefully acknowledges the call "2012-Iniziative di cooperazione universitaria" of the University of Padova, and the Indian Insitute of Technology of Roorkee, especially Dr. R.Chatterjee. Part of the paper is based on a former review papers [19].

References

[1] F. Iachello, Phys. Rev. Lett. 85, 3580 (2000)
[2] F. Iachello, Phys. Rev. Lett. 87, 052502 (2001)
[3] L. Fortunato, Eur. Phys. J. A 26, s01 1-30 (2005)
[4] L. Prochniak, S.G. Rohoziński, J. Phys. G Nucl. Part. Phys. 36, 123101 (2009)
[5] P. Cejnar, J. Jolie and R.F. Casten, Rev. Mod. Phys. 82 (3) 2155-2212 (2010)
[6] F. Iachello, Phys. Rev. Lett. 95, 052503 (2005)
[7] B.F. Bayman and L. Silverberg, Nucl. Phys. 16, 625 (1960)
[8] C.E. Alonso, J.M. Arias, L. Fortunato and A. Vitturi, Phys. Rev. C 72, 061302 (2005)
[9] M. Böyükata, C.E. Alonso, J.M. Arias, L. Fortunato and A. Vitturi, Phys. Rev. C 82, 014317 (2010)
[10] C.E. Alonso, J.M. Arias and A. Vitturi, Phys. Rev. C 75, 064316 (2007)
[11] C.E. Alonso, J.M. Arias, and A. Vitturi, Phys. Rev. Lett. 98, 052501 (2007)
[12] C.E. Alonso, J.M. Arias, L. Fortunato and A. Vitturi, Phys. Rev. C 79, 014306 (2009)
[13] I. Inci, C.E. Alonso, J.M. Arias, L. Fortunato and A. Vitturi, Phys. Rev. C 80, 034321 (2009)
[14] M.S. Fetea *et al.*, Phys. Rev. C 73, 051301(R) (2006)
[15] F. Iachello, A. Leviatan, D. Petrellis, Phys.Lett.B 705 (2011) 379-382; F.Iachello, RIVISTA DEL NUOVO CIMENTO Vol. 34, N. 10, 617-642 (2011)
[16] R.Fossion, C.E. Alonso, J.M. Arias, L. Fortunato and A. Vitturi, Phys. Rev. C 84, 014326 (2011)

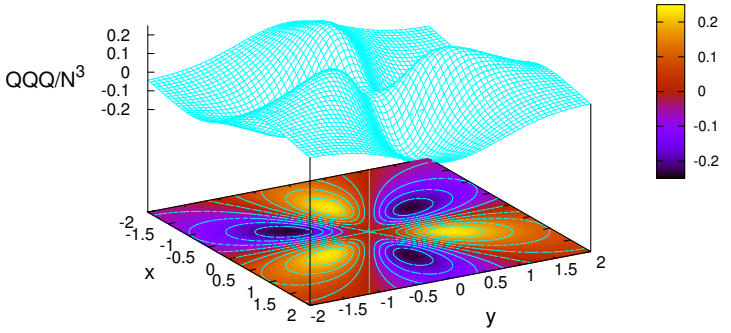

FIG. 9: Surface and contours representing $(\hat{Q}\times\hat{Q}\times\hat{Q})^{(0)}/N^3$ in the large N limit with $\chi = 0$ as a function of the coordinates on the plane ($x = \beta\cos\gamma$ and $y = \beta\sin\gamma$).

[17] L.Fortunato, C.E. Alonso, J.M. Arias, J.E. García-Ramos and A. Vitturi, Phys. Rev. C 75, 064316 (2007)
[18] A.Giannatiempo, L.Fortunato and A.Vitturi, Phys.Rev. C 86, 034311 (2012)
[19] C.E. Alonso, J.M. Arias, L. Fortunato and A. Vitturi, J.Phys.Conf.Ser. 168 (2009) 012011; C.E. Alonso, J.M. Arias, L. Fortunato, M. Böyükata, and A. Vitturi, Int.J.Mod.Phys.E, Vol. 20, No. 2 (2011) 207212